Behavior of superconductivity in a Pb/Ag heterostructure

Hyoungdo Nam, Chendong Zhang, Woojoo Lee, Siyuan Zhu, Hong-Jun Gao, Qian Niu, Gregory A. Fiete, and Chih-Kang Shih

Phys. Rev. B **100**, 094512 — Published 6 September 2019

DOI: 10.1103/PhysRevB.100.094512

Behavior of superconductivity in a Pb/Ag heterostructure

Hyoungdo Nam[1], Chendong Zhang[1,2] , Woojoo Lee[1], Siyuan Zhu[1], Hong-Jun Gao[2], Qian Niu[1], Gregory A. Fiete[1], and Chih-Kang Shih[1,*]

[1]*Department of Physics, The University of Texas at Austin, Austin, Texas 78712, USA.*
[2]*Institue of Physics & University of Chinese Academy of Sciences, Chinese Academy of Sciences, Beijing 100190, China.*
**Corresponding author: shih@physics.utexas.edu*

The superconducting proximity effect is a long-standing topic of great importance in condensed matter physics. A crucial but unresolved issue is which interfacial and material details determine the efficiency of the proximity effect. In this work, we study an epitaxially grown superconductor (SC)/normal metal (NM) heterostructure (Pb/Ag) and find a spatially constant superconducting gap determined by local tunneling spectroscopy and magneto response measurements, despite the highly mismatched Fermi surfaces between individual Pb and Ag epitaxial layers, and the large differences in the lattice constants and electronic density of states in the separate components. The uniform superconducting gap is in contrast to the spatially varying pair potential with a discontinuity at the interface theoretically predicted for an ideal SC-NM junction and experimentally observed previously in several lateral SC-NM junctions. We experimentally verify that the transmission of electrons across the interface in the vertical Pb/Ag heterostructure is high enough that a new band structure emerges even at the single particle level. Our experimental results call for further theoretical work in

order to develop predictive power for the proximity effect starting from realistic, material relevant microscopic models.

When a superconductor (SC) is electronically coupled to a non-SC, it can induce superconductivity in the otherwise non-superconducting region within a length scale of the order of the coherence length [1-12]. This is known as the "proximity effect". Similarly, a non-SC can suppress the superconductivity in a SC over a length scale on the order of the coherence length. The investigation of the proximity (and inverse) effect has been a subject of great interest in condensed matter physics, with recent effort focused on using the superconducting proximity effect to create a platform to harbor exotic Majorana states potentially useful in topological quantum computation [13-21].

As the name "proximity" indicates, this is an induced effect across the SC/non-SC interface. The interface must play a crucial role in determining the efficiency of such coupling. Yet, the precise, material-specific details for a strong proximity effect remain experimentally and theoretically unclear, though conjectures such as Fermi surface alignment have been proposed as a critical factor [17, 19, 20, 22]. Among different SC/non-SC systems, the superconductor/normal metal (SC/NM) system is one of the oldest and most thoroughly investigated. However, the majority of the experimental studies have been carried out using cryo-condensation thin films [4, 8, 9]. Such cryo-quenched films are highly disordered with extremely short electron mean free paths. In addition, their granular nature leads to a less well-defined interface, making it more difficult to understand the role of the interface in the proximity/inverse effect.

Recent advancements in epitaxial growth of superconducting and non-superconducting metallic films with atomic precision have opened up new opportunities to investigate the physics of the interface on the coupling efficiency in the proximity effect (and its inverse). More specifically, as the Fermi surface of individual layers can be tuned with the thickness, the role of Fermi surface matching and the individual electronic density of states can be directly assessed. The SC/NM system that we study in this paper is the Pb/Ag heterostructure grown on Si(111) using molecular beam epitaxy where the quantum well states (QWS) in Pb and Ag layers can be individually tuned [23-26]. The superconductivity is probed using a local probe (scanning tunneling microscopy/spectroscopy) as well as a global probe (double coil mutual inductance)--both applied *in-situ* on the same sample--and they reveal the same superconducting transition temperature, T_c. Moreover, both Pb/Ag and its reverse Ag/Pb heterostructures are grown so that the tunneling gaps (Δ) can be measured on both ends, allowing a rare opportunity to access the spatial dependence of the gap across the interface. We found that Pb/Ag heterostructures behave as a single electronic system, rather than a 2-component system. Astonishingly, we found a uniform gap value persists through the Pb/Ag interface. By contrast, on a *lateral* junction formed from Pb 2D islands and a wetting layer, clear spatial variation of the tunneling gap, $\Delta(r)$, can be observed with an apparent discontinuity across the interface. Such profoundly different behaviors are attributed to the nature of the interface.

Shown in Fig. 1(a) is the scanning tunneling microscopy (STM) image of a Ag film of 9 ML epitaxially grown on Si(111) exhibiting a smooth topography containing only monolayer fluctuations (including such a fluctuation, the average thickness is ~ 9.4 ML for this image). In such a smooth surface the step structure of the underlying Si substrate is also observed. The thickness of the Ag film can be determined by using *in-situ* angled resolved photoemission

(ARPES) to measure the quantum well states (QWS) in the valence band whose energy locations depend very sensitively on the thickness [27, 28]. Shown in Fig. 1(c) is the result for a 14 ML-Ag film. On top of atomically smooth Ag films, Pb is grown subsequently (see Fig. 1(b)). On such Pb films, QWS are readily observable using scanning tunneling spectroscopy (STS) and can be used to determine the thickness of the Pb film unambiguously (Fig. 1(d)) [29]. The observation of QWS on Pb films also signifies an atomically sharp Pb/Ag interface. Using these methods, the thicknesses of Ag and Pb films can each be controlled with single atomic layer precision. In this work, all layer counts include the interfacial wetting layer on Si substrate. We ignore the T_c oscillations due to quantum confinement [25, 30] because its oscillation amplitude is small (~ 0.1 K) when the thickness is larger than 5 ML.

The Δ values were measured *in-situ* using STS as a function of temperature. Shown in Fig. 2(a) is the result for 30 ML-Pb on 10 ML-Ag/Si, exhibiting Bardeen-Cooper-Schrieffer (BCS) quasiparticle-density-of-states (QP-DOS). The fitted $\Delta(T)$ is shown in Fig. 2(b). The BCS fit (back dash line) to the experimental data of $\Delta(T)$ at finite temperatures gives three important values of superconductivity in the sample, such as Δ at zero temperature, Δ_0, the transition temperature of Δ, $T_{c,\Delta}$, and $2\Delta_0/k_BT_c$, reflecting the electron-phonon coupling strength. Detailed discussion of the coupling strength transition is provided in the supplementary information [31], which had been reported previously by O. Bourgeois *et al*. [6].

Shown in Figure 2(c) is an *in-situ* mutual inductance measurement [32] as a function of temperature on the same 30 ML-Pb on 10 ML-Ag/Si. The mutual inductance is strongly correlated with the sheet conductance of a SC film of a thickness d, $\mathrm{Y} = (\sigma_1 + i\sigma_2)d$. A superfluid density (SFD) through the film, $n_{SF} \propto \sigma_2$, and the penetration depth λ is related to the

sheet conductance as $\lambda^{-2} \propto \sigma_2$. From the measured mutual inductance, λ is on the order of a few hundred nm, much greater than the film thickness. It should be noted that the measured SFD includes the contribution from the whole sample. Due to demagnetization of a SC against a driving ac-magnetic field, the non-dissipation part of the mutual inductance (blue) rapidly increases from zero and the dissipation part (red) appears as a tiny spike as the temperature falls below $T_{c,SFD}$ [33]. $T_{c,SFD}$ in Fig. 2(c) is around 5.5 K, which is consistent with $T_{c,\Delta}$ in Fig. 2(b). It signifies that the phase rigidity is well-maintained in the films. The fact that the dissipation component (*i.e.* σ_1) is observed only in a very narrow temperature range near T_c is also consistent with the assessment that phase fluctuation is negligible [34].

Both microscopic and macroscopic T_cs are consistent for all Pb-thicknesses up to L_{Pb} = 50 ML (Fig. 2(d)), confirming long range order of the SC phase. Similar sequences are then carried out with different thicknesses of the underlying Ag films, as shown in Fig. 2(e). (Note that in the case of a zero Ag film thickness, the transition temperature of the Pb film varies as a function of the Pb film thickness.) Also shown as a solid curve is a theoretical fit with

$$T_c(d_{Pb}, d_{Ag}) = T_{c,\infty} e^{-w^*/x}, where\ x = d_{Pb}/d_{Ag}. \quad (1)$$

As shown in Fig. 2(e), a single parameter of $w^* = 0.87$ accounts for all our experimental observations. We emphasize that Eq.(1) breaks down in the limit where d_{Ag} approaches zero since this would imply that even a one or two layer Pb film will approach the bulk T_c, which is clearly not the case [26]. In our case, we found that Eq.(1) holds when $d_{Ag} \geq 5ML$ (1.2 nm). Note that the exponential scaling of T_c with respect to d_{SC}/d_{NM} is a well-known phenomenon

for the SC/NM bilayer system in the Cooper limit (when the thicknesses of SC and NM are smaller than the coherence length) and has been reported in previous studies of SC/NM bi-layer systems fabricated using the cryo-quenched method, albeit with a much smaller scaling coefficient in the exponents, with w^* ranging from 0.2 to 0.6 [7-9]. A larger w^* represents a higher proximity coupling efficiency between epitaxial Pb and Ag. One might consider that this higher coupling efficiency is due to the existence of a cleaner interface, but this would imply the electronic structure of the individual Pb and Ag is unimportant: The Fermi surfaces of individual Pb and Ag layers are comprised of concentric Fermi rings. If the electronic structures of the Pb and Ag layers remain the same as before the heterostructure is formed, then there will be an issue of Fermi surface mismatch between Pb and Ag layers in the thin film regime. However, as we discuss below, the high transmission coefficient of the electron wavefunction across the interface makes it necessary to consider the heterostructure as a whole, albeit metallurgically there is a clear separation between the two.

The STS is applied *locally* on the "surface" of the Pb-side of the Pb/Ag heterostructure. On the other hand, the double-coil measures *the macroscopic* response of the supercurrent for the whole film, which is important since the gap parameter decays as a function of normal film thickness. *Yet both measurements yield the same* T_c. One interesting question arises: What is the spatial dependence of $\Delta(\mathbf{r})$ along the vertical direction? In order to address this question, we create a *reverse heterostructure* with the Ag epitaxial layer on top of the epitaxial Pb film. Shown in Fig. 3(a) is the SFD measurement for a reverse heterostructure with L_{Ag} = 7 ML and L_{Pb} = 21 ML, exhibiting a T_c of 5.4 ± 0.1 K. Note that this value is very similar to the forward heterostructure with L_{Pb} = 30 ML and L_{Ag} = 10 ML (with a T_c of 5.5 ± 0.1 K). Again, this affirms that the T_c is primarily determined by the thickness ratio of d_{Pb}/d_{Ag}. In Fig. 3(b) we show the

tunneling spectra of the forward Pb/Ag (30/10) and the reverse Ag/Pb (7/21) heterostructures acquired at 2.2 K. The Δ can be fitted very well with the standard BCS QP-DOS function with fitted gap values of Δ=1.12 meV and Δ= 1.07 meV, respectively. Thus, within the experimental error bar, the two gap values are essentially identical, indicating that *the gap is uniform along the vertical direction across the interface without any discontinuity*. Additional sets of reverse heterostructures (with d_{Ag} ranging from 6 to 10 MLs at d_{Pb} = 16 MLs) have been investigated (see supplementary Fig. S6 [31]). Shown in Figure 3(c) are results for forward vs reverse heterostructures whose T_c are deduced from measurements of Δ *vs T*. In all cases, the conclusion remains the same – both forward and reverse heterostructures, yield similar Δ(T) values for the same d_{Pb}/d_{Ag}.

This raises another interesting question. According to de Gennes [5], the pairing potential $\Delta(\mathbf{r})$ is spatially varying and in general contains a discontinuity across the SC-NM interface (see the schematic shown in Fig. 3(d)). Experimentally, several recent works using STM to visualize $\Delta(\mathbf{r})$ across the lateral SC/NM heterostructures indeed upheld this prediction [10-12]. In Fig. 3(e) we reproduce a result for a lateral junction comprised of a 5 ML-Pb island and the surrounding wetting layer on the Si substrate, which is fabricated by depositing Pb on directly Si and leads to small Pb islands that exhibit a weak proximity effect in the Si (in stark contrast to the Pb/Ag structure). In addition to a spatially varying $\Delta(\mathbf{r})$, one sees that a discontinuity is established within ~ 1 nm at the interface, agreeing with the theoretical description shown in Fig. 3(d).

Why does the epitaxial Pb/Ag planar vertical junction exhibit such a distinctly different behavior? If one treats the SC and NM as two electronically distinctive regions then a self-consistent solution to the Bogoliubov-de Gennes equation indeed shows a spatial varying $\Delta(\mathbf{r})$

like the one in Fig. 3(c). The gap in the NM region is "induced" via the proximity effect. Note that the discontinuity occurs within a length scale < 1 nm. At the single particle level, if one treats the Pb and Ag regions as two electronically distinct thin films, then the mismatch in Fermi wave vectors of the QWS in the two regions would significantly impede the electronic coupling between the two regions. Below we resolve these issues by considering that the two regions are *not* electronically distinct even at the single particle level.

Previously, M. K. Brinkley *et al*. have used ARPES to show that in the epitaxial Pb/Ag on Si(111), Ag-like QWS can be observed even with a Pb overlayer as high as 25 ML (much thicker than the escape depth of photoelectrons) [35]. They argue that this is evidence that the electrons in the Ag layer maintain their coherence as they traverse through the Pb overlayer during the photoemission process. Here we take a step further and argue that in the Pb/Ag heterostructures, one should consider the electronic structures as a single system even at the single-particle level, leading to the formation of a new set of QWS. Shown in Figures 4(a)-(c) are QWS observed using ARPES for (i) a 9 ML-Ag film on Si, (ii) with an additional 10 ML-Pb on top of the 9 ML-Ag, and (iii) a 10 ML-Pb film on Si, respectively. Also shown in Fig. 4(d) are respective spectra at $k = 0$ where we also label QWS in individual layers by vertical arrows (in Ag, surface states is marked as SS). The individual Ag and Pb QWS are consistent with previous reports, including the observation fringes (marked by "*" in Fig. 4(d)) due to the quantized hole states of the Si surface resulting from the formation of Schottky barrier). The QWS and their dispersions in the heterostructure (Fig. 4(b)), however, do not resemble those of Ag QWS (Fig. 4(a)), nor Pb QWS (Fig. 4(c)), nor their superpositions. In Ag and Pb regions the QWS are regularly spaced. In the heterostructure, the QWS are not evenly distributed and come in pairs. Moreover, if we compare the QWS #1 in the heterostructure and the QWS #1 in the Pb layer

whose energy locations are close to each other, one finds an entirely different dispersion relationship. Thus, one can safely say that QWS in the heterostructure have their own identities. The schematic in Figure 4(e) illustrates that electrons in Pb and Ag layers are not individually confined. Instead, the quantum confinement is applicable only to the whole heterostructure. Shown in Fig. 4(f) is a model calculation of the QWS of the composite by using a 20 Å/20 Å model heterostructure with free-electron like states of different effective masses for Ag and Pb ($m_{Ag} = 0.4 \times m_0$ and $m_{Pb} = 1.0 \times m_0$). The result captures the salient features of our observation: the non-even distribution of QWS whose dispersion also differ from either individual layers. More details of the model calculation can be found in the supplementary material [31]. We emphasize that this model calculation is not intended to provide a quantitative match to the experimental result. A full first-principle calculation would be necessary, which is beyond the scope of this paper. Nevertheless, the experimental evidence is compelling that the Pb/Ag heterostructure has one integral single-particle set of electronic states. Thus, it naturally leads to a constant $\Delta(\mathbf{r})$ across the interface.

In summary, by using epitaxially grown Pb/Ag heterostructures on Si, we show that there is a spatially constant pairing potential across the interface (in contrast to a lateral SC/NM heterojunction), consistent with the global superfluid density measurement of superconductivity. At the single particle level, we show the existence of a single set of QWS for the whole heterostructure instead of individual QWS for individual layers, removing the restriction of Fermi surface matching at the interface. Our work illustrates the importance of interface engineering in designing mesoscopic system for proximity induced superconductivity, and calls for further theoretical work in order to develop predictive power for the proximity effect starting from realistic, material relevant microscopic models.

Acknowledgements

This work was supported by ONR-N00014-14-1-0330, the National Science Foundation DMR-1506678, DMR-1507621, NSF Materials Research Science and Engineering Center Grant No. DMR-1720595, DMR-1729588, and the Welch Foundation (F-1672). H. -J. Gao acknowledges support by MOST grant No. 2013CBA01601 and by NSFC grant No. 61390501. G.A.F. acknowledges support from a Simons Fellowship and a QuantEmX grant from ICAM and the Gordon and Betty Moore Foundation.

Author contributions

H.N., C.Z. and C.K.S. designed and coordinated the experiments. H.N., C.Z., W.L., and S.Z. carried out the experiments; H.N., C.Z., W.L., S.Z., H.G., Q.N. G.A.F, and C.K.S. analyzed the data; H.N., C.Z., Q.N., G.A.F, and C.K.S. wrote the paper with inputs from other coauthors.

Additional information

The authors declare no competing financial interests.

References

[1] R. Holm, W. Meissner, Z. Phys. **74**, 715 (1932).
[2] H. Meissner, Phys. Rev. **117**, 672 (1960).
[3] L. N. Cooper, Phys. Rev. Lett. **6**, 689 (1961).
[4] P. Hilsch, Zeitshrift fur Physik **167**, 511 (1962).
[5] P. G. de Gennes, Rev. Mod. Phys. **36**, 225 (1964).
[6] O. Bourgeois, A. Frydman, R. C. Dynes, Phys. Rev. B **68**, 092509 (2003).
[7] Z. Long, M. D. Stewart Jr., T. Kouh, J. M. Valles Jr., Phys. Rev. Lett. **93**, 257001 (2004).
[8] I. Sternfeld, V. Shelukhin, A. Tsukernik, M. Karpovski, A. Gerber, A. Palevski, Phys. Rev. B **71**, 064515 (2005).
[9] S. Bose, P. Ayyub, Phys. Rev. B **76**, 144510 (2007).
[10] J. Kim, V. Chua, G. A. Fiete, H. Nam, A. H. MacDonald, C.-K. Shih, Nature Phys. **8**, 464 (2012).
[11] L. Serrier-Garcia, J. C. Cuevas, T. Cren, C. Brun, V. Cherkez, F. Debontridder, D. Fokin, F. S. Bergeret, D. Roditchev, Phys. Rev. Lett. **110**, 157003 (2013).
[12] H. Kim, S. Z. Lin, M. J. Graf, Y. Miyata, Y. Nagai, T. Kato, Y. Hasegawa, Phys. Rev. Lett. **117**, 116802 (2016).
[13] L. Fu, C. L. Kane, Phys. Rev. Lett. **100**, 096407 (2008).
[14] J. D. Sau, R. M. Lutchyn, S. Tewari, S. Das Sarma, Phys. Rev. B **82**, 094522 (2010).
[15] V. Mourik, K. Zuo, S. M. Frolov, S. R. Plissard, E. P. A. M. Bakkers, L. P. Kouwenhoven, Science **336**, 1003 (2012).
[16] P. Zareapour, A. Hayat, S. Y. F. Zhao, M. Kreshchuk, A. Jain, D. C. Kwok, N. Lee, S.-W. Cheong, Z. Xu, A. Yang, G. D. Gu, S. Jia, R. J. Cava, K. S. Burch, Nature Commun. **3**, 1056 (2012).

[17] E. Wang, H. Ding, A. V. Fedorov, W. Yao, Z. Li, Y.-F. Lv, K. Zhao, L.-G. Zhang, Z. Xu, J. Schneeloch, R. Zhong, S.-H. Ji, L. Wang, K. He, X. Ma, G. Gu, H. Yao, Q.-K. Xue, X. Chen, S. Zhou, Nature Phys. **9**, 621 (2013).
[18] I. K. Drozdov, A. Alexandradinata, S. Jeon, S. Nadj-Perge, H. Ji, R. J. Cava, B. A. Bernevig, A. Yazdani, Nature Phys. **10**, 664 (2014).
[19] S.-Y. Xu, N. Alidoust, I. Belopolski, A. Richardella, C. Liu, M. Neupane, G. Bian, S.-H. Huang, R. Sankar, C. Fang, B. Dellabetta, W. Dai, Q. Li, M. J. Gilbert, F. Chou, N. Samarth, M. Z. Hasan, Nature Physics **10**, 943 (2014).
[20] T. Yilmaz, I. Pletikosić, A. P. Weber, J. T. Sadowski, G. D. Gu, A. N. Caruso, B. Sinkovic, T. Valla, Phys. Rev. Lett. **113**, 067003 (2014).
[21] Q. L. He, L. Pan, A. L. Stern, E. C. Burks, X. Che, G. Yin, J. Wang, B. Lian, Q. Zhou, E. S. Choi, K. Murata, X. Kou, Z. Chen, T. Nie, Q. Shao, Y. Fan, S.-C. Zhang, K. Liu, J. Xia, K. L. Wang, Science **357**, 294 (2017).
[22] J.-H. She, A. V. Balatsky, Phys. Rev. Lett. **109**, 077002 (2012).
[23] A. R. Smith, K. J. Chao, Q. Niu, C. K. Shih, Science **273**, 226 (1996).
[24] Z. Zhang, Q. Niu, C. K. Shih, Physical Review Letters **80**, 5381 (1998).
[25] Y. Guo, Y.-F. Zhang, X.-Y. Bao, T.-Z. Han, Z. Tang, L.-X. Zhang, W.-G. Zhu, E. G. Wang, Q. Niu, Z. Q. Qiu, J.-F. Jia, Z.-X. Zhao, Q.-K. Xue, Science **306**, 1915 (2004).
[26] S. Qin, J. Kim, Q. Niu, C.-K. Shih, Science **324**, 1314 (2009).
[27] I. Matsuda, T. Ohta, H. W. Yeom, Phys. Rev. B **65** (2002).
[28] N. J. Speer, S. J. Tang, T. Miller, T. C. Chiang, Science **314**, 804 (2006).
[29] M. Becker, R. Berndt, Phys. Rev. B **81**, 205438 (2010).
[30] D. Eom, S. Qin, M. Y. Chou, C. K. Shih, Phys. Rev. Lett. **96**, 027005 (2006).
[31] See Supplemental Material at [URL will be inserted by publisher] for coupling strength transition;T-dependent gap measurements for the reverse heterostructure;QWS calculation of a 20 Å-Ag model heterostructure;Quantum well states in Pb film grown on Ag.
[32] H. Nam, P.-H. Su, C.-K. Shih, Rev. Sci. Instrum. **89**, 043901 (2018).
[33] A. F. Hebard, A. T. Fiory, Phys. Rev. Lett. **44**, 291 (1980).
[34] H. Nam, H. Chen, T. Liu, J. Kim, C. Zhang, J. Yong, T. R. Lemberger, P. A. Kratz, J. R. Kirtley, K. Moler, P. W. Adams, A. H. MacDonald, C. K. Shih, Proc. Natl. Acad. Sci. USA **113**, 10513 (2016).
[35] M. K. Brinkley, Y. Liu, N. J. Speer, T. Miller, T.-C. Chiang, Phys. Rev. Lett. **103**, 246801 (2009).

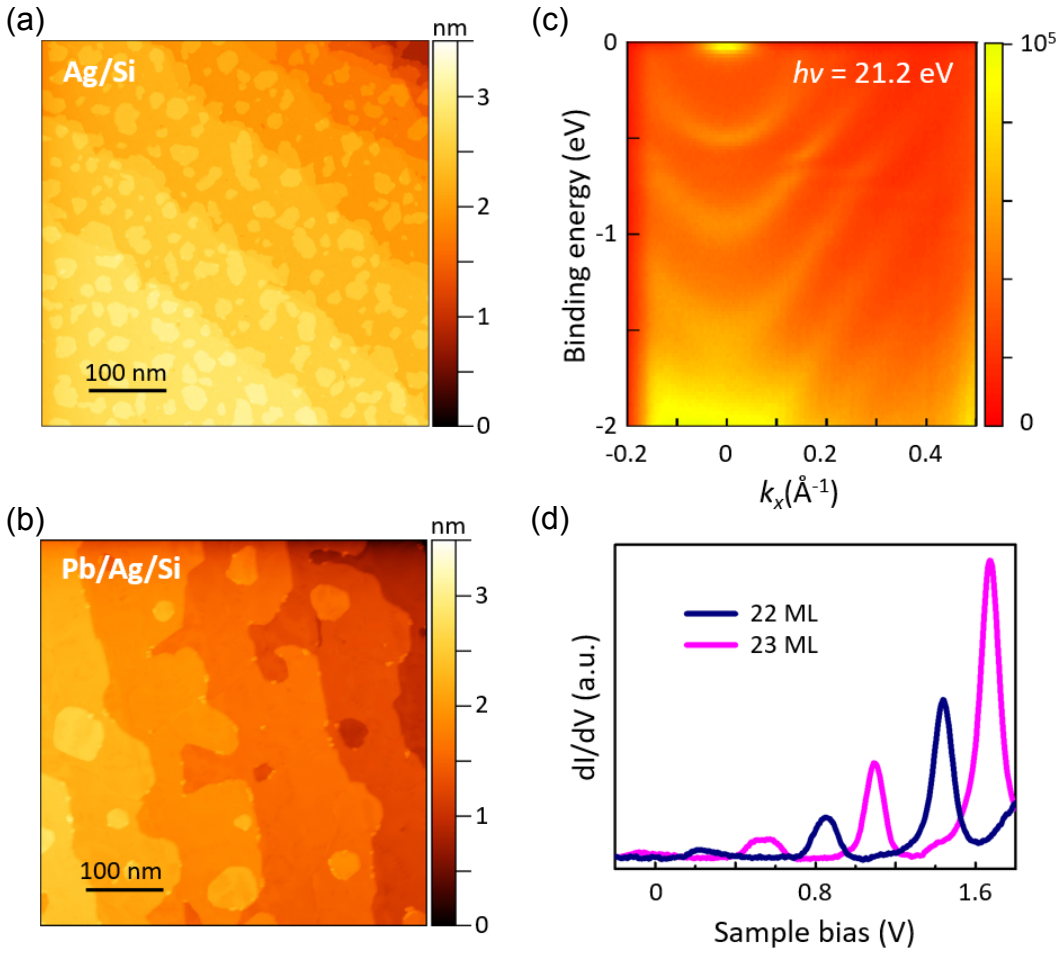

FIG. 1 (color online) Growth of Pb/Ag heterostructure with an atomically sharp interface. (a), (b) STM topography of 9 ML-Ag/Si(111)-7×7 and 22 ML-Pb on top of 7 ML-Ag film, taken at 4.3 K with V_{Sample} = 2 V. (c) ARPES spectrum on 14 ML-Ag/Si(111) at $h\nu$ = 21.2 eV, showing obvious QWS dispersions. (d) Tunneling spectroscopy on 22 ML (blue) and 23 ML (pink) Pb films grown on 7 ML-Ag/Si. The peak locations of QWS are irrelevant to the thickness of underlying Ag film. (See supplementary information [31] for details.)

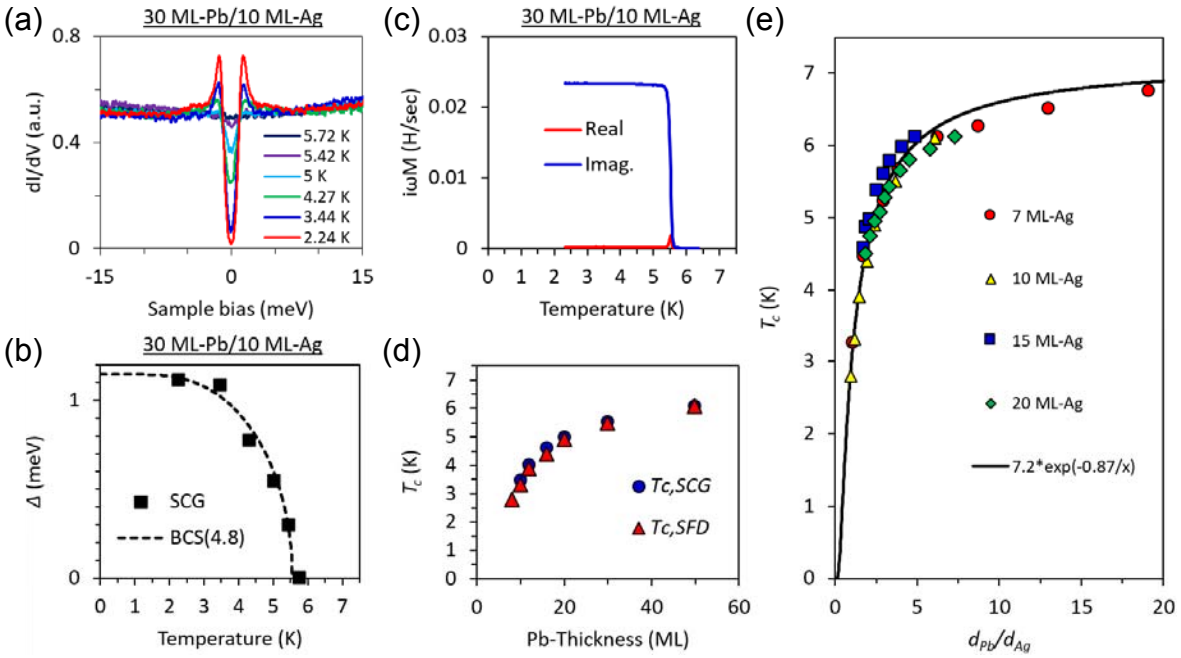

FIG. 2 (color online) Thickness dependence of superconductor transition temperature. (a) in-situ STS on 30 ML-Pb/10 ML-Ag/Si(111). (b) Temperature dependence of Δ(T), deduced from BCS QP-DOS fit to tunneling spectra in (a). Here, the BCS curve (dash) is drawn using $2\Delta_0/k_BT_c$ = 4.8. (c) Mutual inductance measurements on 30 ML-Pb/10 ML-Ag/Si(111). (d) On 10 ML-Ag/Si, Pb-thickness dependence of T_c . $T_{c,SCG}$ and $T_{c,SFD}$ are obtained by STS and SFD, respectively. (e) Transition temperature as a function of thickness ratio of d_{Pb}/d_{Ag} for different thicknesses of underlying Ag films. The black solid line of $7.2 \times e^{-0.87\frac{d_{Ag}}{d_{Pb}}}$ is the fit based on an average pairing model [3].

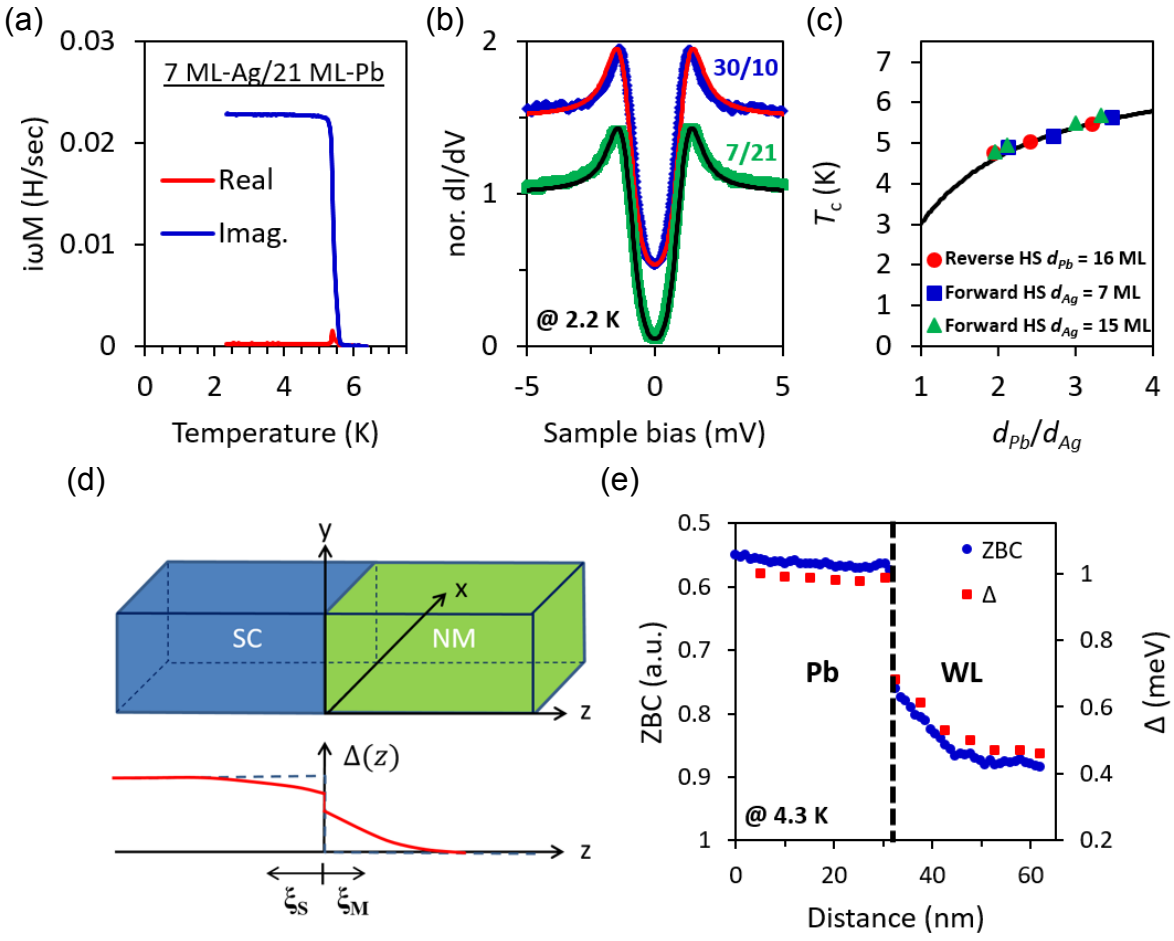

FIG. 3 (color online) Inverse heterostructure and lateral SC-NM junction. (a) Mutual inductance measurement of 7 ML-Ag on 21 ML-Pb/Si(111). (b) Tunneling spectrum of 7 ML-Ag/21 ML-Pb (green square) at 2.2 K, compared with one of 30 ML-Pb/10 ML-Ag (blue rhombus) and BCS QP-DOSs (solid lines). Both heterostructures have the same thickness ratio of L_{Pb}/L_{Ag} = 3. (For clarity, there is 0.5 offset.) T_c in (a) is consistent with Fig. 2(e). Pb/Ag and its inverse heterostructures show the same Δ within the experimental error bar. (c) Comparison of T_c as a function of d_{Pb}/d_{Ag} for forward and reverse heterostructure. Here T_c are deduced from measurements of Δ *vs* T. (d) Schematic of SC-NM junction and tunneling gap profile along z-axis perpendicular to the interface. (e) Zero bias conductance (ZBC) profile showing the discontinuous transition at the boundary between 5 ML-Pb island and the surround wetting layer as the theoretical description (d).

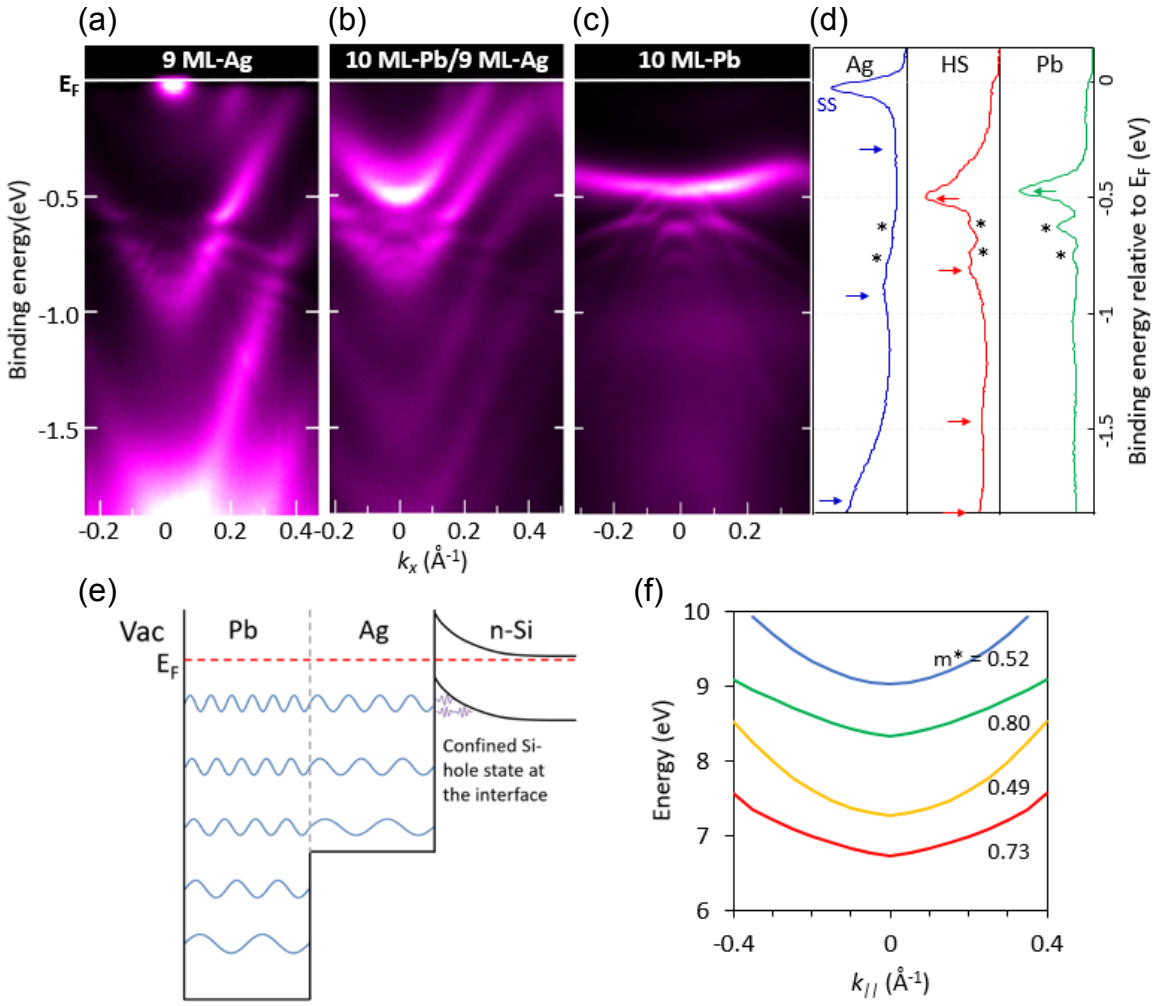

FIG. 4 (color online) One integral single particle electronic states of Pb/Ag heterostructure. (a)-(c) ARPES spectra of a 9 ML-Ag film on Si (a), an additional 10 ML-Pb on top of 9 ML-Ag (b), and a 10 ML-Pb film on Si (c). (d) Spectra at k = 0 for Ag, Ag/Pb heterostructure, and Pb layers respectively. (e) Schematic of Pb/Ag heterostructure as a one integral single particle system crossing Pb/Ag interface. (f) The model calculation of the QWS of (d) by using a 20 Å/20 Å model heterostructure with free-electron like states of $m_{Ag} = 0.4 \times m_0$ and $m_{Pb} = 1.0 \times m_0$ for Ag and Pb, respectively. This result captures the new QWS formation and pairing feature in (b), which come from the one single particle electronic state of Pb/Ag heterostructure. Note that in addition to the QWSs being observed, one can see interference fringes between QWSs and a downward hole-like dispersive Si states at the interface. Such features have been reported and

discussed in details by N. J. Speer, et al. [28] for the Ag/Si case. Here we observed such interference fringes in cases of Pb/Ag/Si and Pb/Si. This provides addition evidence that Pb/Ag heterostructures form one coherent electronic system which also experience the presence of Si states at the interface (just like the Ag QWSs).